16TH EUROPEAN CONFERENCE ON EARTHQUAKE ENGINEERING THESSALONIKI 18 - 21 JUNE 2018

FIRE-AFTER-EARTHQUAKE BEHAVIOUR OF INDUSTRIAL FACILITIES WITH FIRE PROTECTED STEEL STRUCTURAL SYSTEM

Kalliopi ZOGRAFOPOULOU[1], Daphne PANTOUSA[2], Euripidis MISTAKIDIS[3]

ABSTRACT

Passive fire protection of steel structures with requirements over 2 hours is usually achieved by the application of cementitious Sprayed Fire Resistive Materials (SFRM). These materials exhibit brittle behaviour which, in addition to their low mechanical strength, can result in severe damage to the fire protection when the structural elements undergo substantial deformations, such as in the position of plastic hinges, during an earthquake event. This damage can pose a threat to the stability of a structure in the event of a fire, which is a common occurrence after an earthquake. In this study, a structure designed according to the current codes for earthquake and fire is submitted to these events and the damage occurring to the fire protection around the plastic hinge of a beam with its consequential effect on the temperature distribution in the steel member is evaluated. A 3D numerical model of the SFRM protected beam is submitted initially to cyclic loading equivalent to the design earthquake load of the considered structure, and the damage of the fire protection around the plastic hinge is obtained. Subsequently, a thermal model of the damaged beam is submitted to 2 hours ISO-834 loading and the resulting temperature field is compared to the one of the undamaged and uninsulated steel section.

Keywords: Fire-after-Earthquake; Cementitious SFRM; Steel; Damage

1. INTRODUCTION

The fire protection study of industrial facilities includes both active and passive protection measures. In the case of steel structural systems, usually fire protection coatings are employed. For moderate fire protection demands, intumescent coatings are used. However, for higher fire protection demands (e.g. more than 2 hours) cementitious coatings are used. The latter, are usually sprayed directly on the finished steel structure. The European design recommendations contain procedures for the calculation of the critical temperatures of steel members, without specifying how these temperatures can be assured, i.e. it is in the hands of the designer and/or the contractor to decide the specific type of fire protection coating to be used for a specific application. Recently experimental studies (Chen et al.,2014, Braxtan and Pessiki,2011) started providing alarming evidence on the behaviour of steel members with cementitious fire protection coating in monotonic and cyclic loading. More specifically, it was verified that under intense static loading reaching the levels of steel yielding, significant damage arises in the fire protection coating, posing questions for its subsequent fire behaviour. The situation is even worst in case of cyclic loading, in which, even for rather low displacement amplitudes significant damage occurs in the coating, leading to extended steel areas exposed to a possible fire.

On the other hand, the occurrence of fire after an earthquake (FAE) event, is something that has been witnessed many times in recent years (Northridge 1994, Kobe 1995, Chile 2010, Tohoku 2011). In such cases, urban environment characteristics (gas piping system, electricity wiring system, etc.) and

[1]Doctoral Candidate, Dept. of Civil Engineering, University of Thessaly, Volos, Greece, kazograf@gmail.com
[2] Research Fellow, Faculty of Engineering and the Environment, University of Southampton, Southampton, UK, D.Pantousa@soton.ac.uk
[3]Professor, Dept. of Civil Engineering, University of Thessaly, Volos, Greece, emistaki@gmail.com

post-earthquake conditions (multiple ignition points, malfunction of the active fire-protection systems, etc) were combined and the fire that followed the seismic event became the predominant cause of damage, disruption of building use and occupation, injuries, and loss of human life. Research work on the behaviour of steel frames under FAE loading is limited but provides strong evidence that fire resistance is reduced when the steel frame has already experienced seismically induced damage in structural members (Keller, 2012, Faggiano and Mazzolani, 2011, Memari et al., 2014, Pantousa and Mistakidis, 2015). When critical or industrial facilities are affected, the consequence of these fires may also have a significant environmental impact. Note that such facilities are those requiring increased fire protection times, and in which cementitious fire protection coatings are most commonly used. Therefore, a possible damage to the fire protection coating due to the hysteretic behaviour in critical energy dissipation areas of the structural system during earthquakes, creates a significant vulnerability in the case of a subsequent fire, reducing substantially the time that a structure can sustain the fire event. According to the current European design framework, engineers are not obliged to consider such phenomena, hence increasing the possibilities of catastrophic events.

The present paper tries to quantify the consequences of fire-after-earthquake events in structures in which cementitious coatings have been used for the fire protection. In the first part of the paper, a steel moment resisting frame is designed for gravity and seismic loading according to the guidelines of EN 1993-1-1 (2005) and EN 1998-1-1 (2004). The seismic behaviour of the building is assessed through dynamic transient analysis with direct integration of the equations of motion. The damage induced in steel beams is calculated using a damage index available in the literature. The second part of the study is focused on the local behaviour of sprayed cementitious fire protection coatings. To this end, experiments on fire protected steel plates are reproduced numerically, through advanced three-dimensional finite element models, in order to understand the mechanisms that lead to the damage of the fire protection coating and the corresponding failure modes. Highly nonlinear phenomena are taken into account, such as cracking and crushing of the cementitious coating, delamination that develops on the steel-coating interface, etc. Then, the results yielded by the numerical tests are used in order to reproduce the behaviour of fire protected standard IPE steel beam of the moment resisting frame in bending, causing the development of plastic hinges, therefore simulating the effects of earthquake loading. Specifically, cyclic loading is introduced in order to induce damage at the beam and this loading leads to the same damage index that is defined in the first part of the study. Detailed three dimensional models employing solid finite elements are also used in this respect. The damaged models are in the sequel submitted in thermal loading, in order to study the effect of coating damage on the temperatures that develop in the steel material, under standard ISO fire (gas temperatures).

2. CEMENTITIOUS SPRAYED FIRE RESISTIVE MATERIALS (SFRM)

Cementitious Sprayed Fire Resistive Materials (SFRM) are mixtures based on cement, gypsum, vermiculite and perlite which due to their low thermal conductivity are used as a fire protective coating that is sprayed directly on the surface of steel structural members. In addition to their thermal behaviour, their low weight and relatively low cost, compared to intumescent coatings, has led to their wide use in steel structures, especially in constructions of larger scale, such as industrial facilities, which require high values of fire resistance, usually over 2 hours. Their main disadvantage, however, is that, due to their particular composition, they exhibit brittle behaviour, which is accompanied by low mechanical strength. Typical values for the tensile strength of these mixtures are in the range of 0.05 MPa and for the compressive strength in the range of 0.59MPa. The interfacial bond between SFRM materials and steel is also quite low at 0.04MPa in the normal direction and 0.07MPa in the tangential one (Chen et al., 2010).

The structural performance of cementitious SFRM applied on steel plates under tensile, compressive and flexural loading, has been tested experimentally by Chen et al. (Chen et al., 2014). The test results showed that under axial tensile loading of the steel plate, interfacial cracks formed at both ends of the coating at steel strains of 0.08%-0.12%, propagating gradually towards the center of its length, until transverse cracks formed which stopped the further cracking at the interface, while getting wider as the

tensile load increased. Under axial compressive loading of the SFRM covered steel plate, interfacial cracks formed at both ends of the SFRM coat at steel strain levels of 0.2%, propagating towards the center of the length of the specimen, which delaminated completely when the steel strain reached 0.3% without any internal damage. The same modes of failure were observed in the flexural tests of SFRM covered steel plates, on the tension and compression side respectively. On the tension side the cementitious coating, initially interfacial cracks formed at both ends, and with further loading the propagation of the interface failure was stopped by the formation of transverse cracks, dividing the coating into several segments, that remained attached to the steel plate. On the compression side, interfacial cracks, which initiated at both ends, spread towards the center, where a transverse crack developed in the small area still attached to the plate because of the large curvature of the plate. It was established that two main mechanisms govern the failure of the cementitious SFRM coatings, a) interfacial cracking and debonding of the coating from the steel plate and b) structural failure of the coating itself, due to its low mechanical resistance.

3. MOMENT RESISTING FRAME UNDER EARTHQUAKE LOADING

The study is focused on a typical steel frame of an industrial building as it is presented in Figure 1a. The loads (permanent and live) that are considered according to EN 1991-1-1(2002) for the design of the industrial building, are 15kN/m and 9 kN/m for the permanent and the live loads respectively. The seismic design of the structure is conducted according to EN 1998-1-1 (2004). For the needs of this study, the seismic action is represented through the elastic response spectrum of Type 1. The soil type is classified as B. The design ground acceleration α_g is taken equal to 0.36 g. The design spectrum that is used in this study takes into account a behaviour factor q equal to 4. The selected cross-section of the structural members are illustrated in Figure 1a.

Primary results are obtained through a push-over analysis, in order to determine the capacity of the system in terms of base-shear and roof displacement, and the plastic hinge mechanism. The capacity curve of the frame is pressed in Figure 1b. Also, the plastic hinge mechanism of the structure reveals that the plastic hinges are formed at the ends of the beams and at the bases of the columns. This follows the requirements of the capacity design of the structural system.

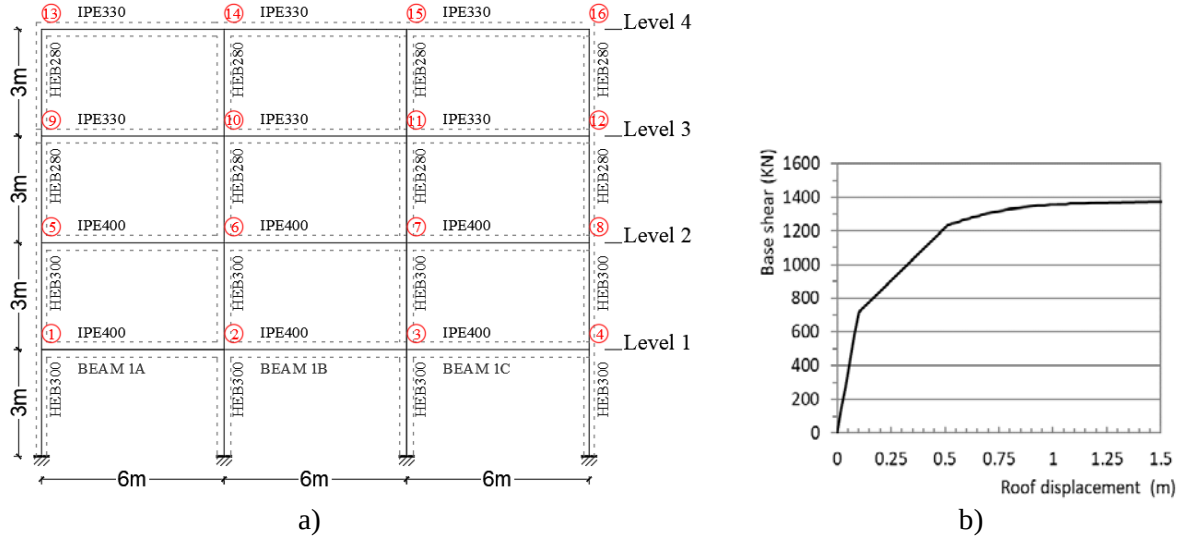

Figure 1. a) The static pushover curve for the steel frame, b) The static pushover curve for the steel frame

Next, the frame behaviour of the frame structure is obtained, using dynamic transient analysis with direct integration of the equations of motion. The Hiber – Hughes – Taylor method is used and the time step is set equal to 0.001s. The seismic action is simulated through the accelerogram that is presented in Figure 2. The accelerogram is scaled according to EN 1998-1-1 (2004) in order to match the elastic spectrum. The numerical model is developed using the Finite Element code SAP2000

(2017) and the yield stress of the structural steel is assumed to be equal to 275MPa for the beams and S325 for the columns of the frame. In order to simplify the calculations, isotropic hardening is considered. The dissipated energy of the structure during the earthquake excitation is modeled through the Rayleigh damping type.

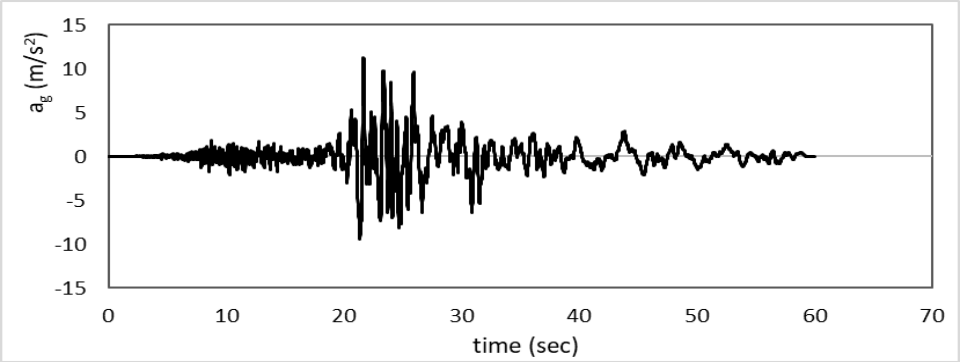

Figure 2. The accelerogram used for the non-linear time- history analysis

The results of the analysis in terms of the moment-rotation curve of beam 1a, as it is indicated in Figure 1a are presented in Figure 3. The damage that is induced in the structural member is calculated according to the damage index that is proposed by Krawinkler (Krawinkler, 1981 , Krawinkler and Zohrei, 1983, Castiglioni and Pucinotti, 2009). This damage index is based on cumulative plastic deformation and accounts for the different weight of the plastic deformation of the various cycles. Finally, the damage index is found to be equal to 44.54.

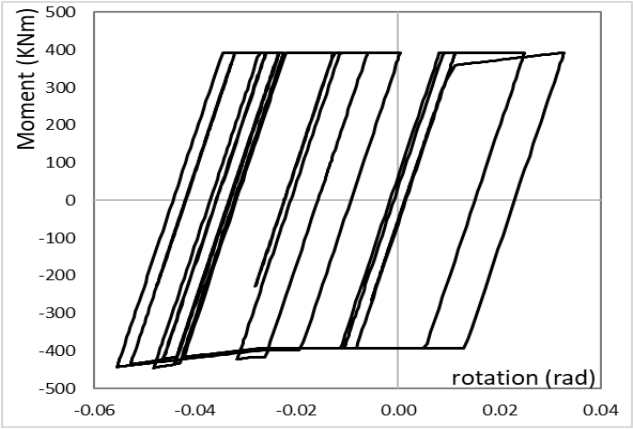

Figure 3. The moment rotation curve for joint 1 of the steel frame

4. NUMERICAL ANALYSIS OF CEMENTITIOUS SFRM DAMAGE ON STEEL MEMBERS

4.1 Numerical Simulation of SFRM Coated Steel Plates Under Bending Load

In a previous study by the authors (Zografopoulou and Mistakidis, 2017), a simulation of the failure modes of the SFRM coating during the flexural test was conducted, and the behaviour of the SFRM coating was numerically reproduced.

The numerical model consisted of a steel plate which had a layer of cementitious coating on both sides. The model was created by hexahedral solid elements both for the steel and the coating. The material behaviour of the cementitious coating was modelled using the smeared cracking approach. A crack would form perpendicular to the maximum stress plane when the stress exceeded the tension strength of the material. After the formation of a crack the stress curve follows a descending softening

branch until zero stress and after that there is no further load-carrying capacity in tension. In compression, the stress-strain curve is linear until the critical compression stress is reached, followed by a fully plastic branch. Steel was modelled with a standard linear stress-strain curve with hardening. The contact interaction between steel and SFRM coating was modelled using the Yamada-Sun stress criterion (Yamada and Sun, 1978) which has the form:

$$A = \left(\frac{\sigma_n}{S_n}\right)^2 + \left(\frac{\sigma_t}{S_t}\right)^2 \leq 1 \quad (1)$$

where, σ_n is the contact normal stress, σ_t is the tangential contact stress, S_n is the normal bonding strength, S_t is the shear bonding strength.

The two materials are initially in glue contact, with displacement constraints in all directions. When A=1, the displacement constraints are released, and the two contact bodies can develop relative displacements. The simulation results were similar to the test observations. The cementitious coating on the compression side started cracking at the interface on both ends, then the interface delamination propagated towards the center where the coating finally cracked due to the curvature of the underline steel plate. On the tension side, delamination initiated at both ends, but did not extend much further towards the center, as a result of the formation of multiple transverse cracks along the length of the coating. With further loading, the cracked areas got deeper and wider, but the coating segments remained attached to the steel plate until the end of the simulation. A comparison of the simulation failure modes with the test results is presented in Figure 4.

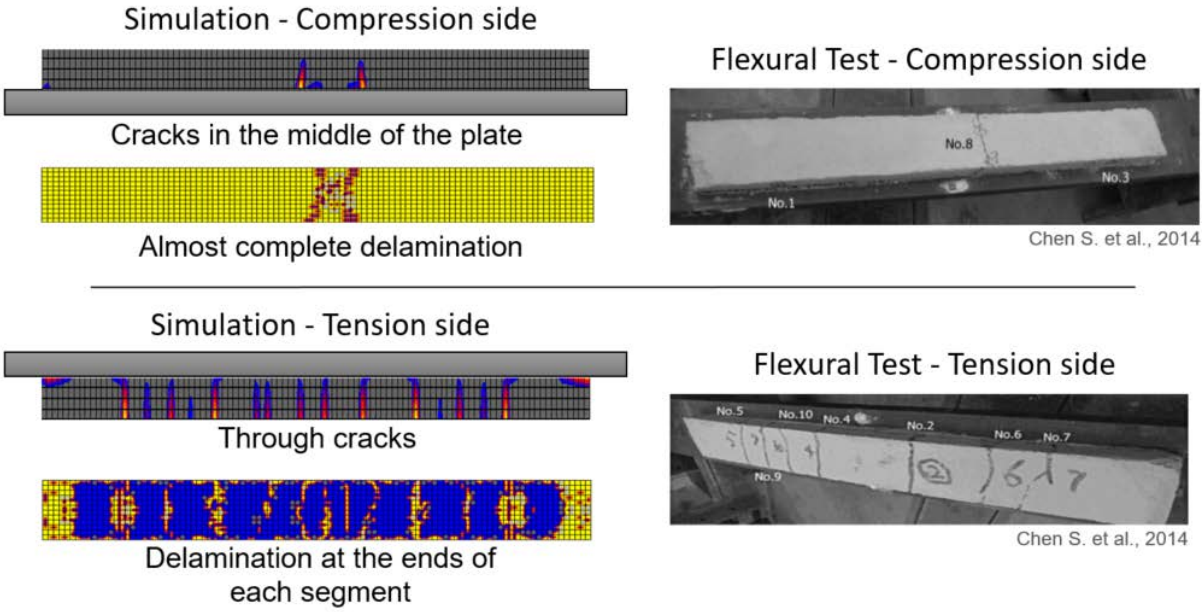

Figure 4. Simulation results and test result comparison on the failure modes of cementitious SFRM coated steel plates under flexural loading

4.2 Numerical Simulation of SFRM Coated Steel Beam Under Cyclic Rotation

In order to study the SFRM damage on a steel structural member under seismic load, the method that was used in the simulation of the flexural test of the SFRM coated steel plate is applied in the modelling of a 6.00 m, IPE 400 steel beam with 25mm cementitious SFRM coating along the cross section perimeter. The beam (Figure 5), which is part of the steel frame, is subjected to cyclic loading (Figure 6) that is applied as imposed rotation on the beam ends, simulating the deformation that would be caused by an earthquake load. The cyclic rotation is applied until a similar value of the damage

index, which was calculated for the same joint in the moment resisting frame subjected to the earthquake excitation, is reached.

The beam and the SFRM coating are simulated by eight-node, isoparametric, arbitrary, hexahedral solid elements. Only a quarter of the beam is simulated, taking into account the symmetry conditions along the xz-plane, and the antisymetric deformation of the beam along the x-axis. The imposed rotation is applied on the beam's end and the necessary boundary conditions are applied on the symmetry plane and at midspan. The material properties of the model are presented in Table 1. The rotation is applied in 3 full cycles with increasing magnitude at the levels of 10, 20 and 30 mrad. Steel is modelled using an elastic-plastic material behaviour. The cementitious SFRM coating is simulated by a smeared crack model. In tension the material develops a crack when the critical tension strength is reached, followed by a tension softening branch until zero stress. When the loading is reversed, the crack closes and is assumed that it has full compressive stress-carrying capability, but with a reduced shear modulus. The interface interaction is modelled using the Yamada-Sun stress criterion given in equation 1. The analysis is contacted using the non-linear structural analysis software MSC-MARC (MSC-MARC, 2014) and takes into account the nonlinearity of the materials and the contact interaction between the two contact bodies. The main goal is to study the failure modes of the cementitious SFRM coating at the position of the plastic hinge.

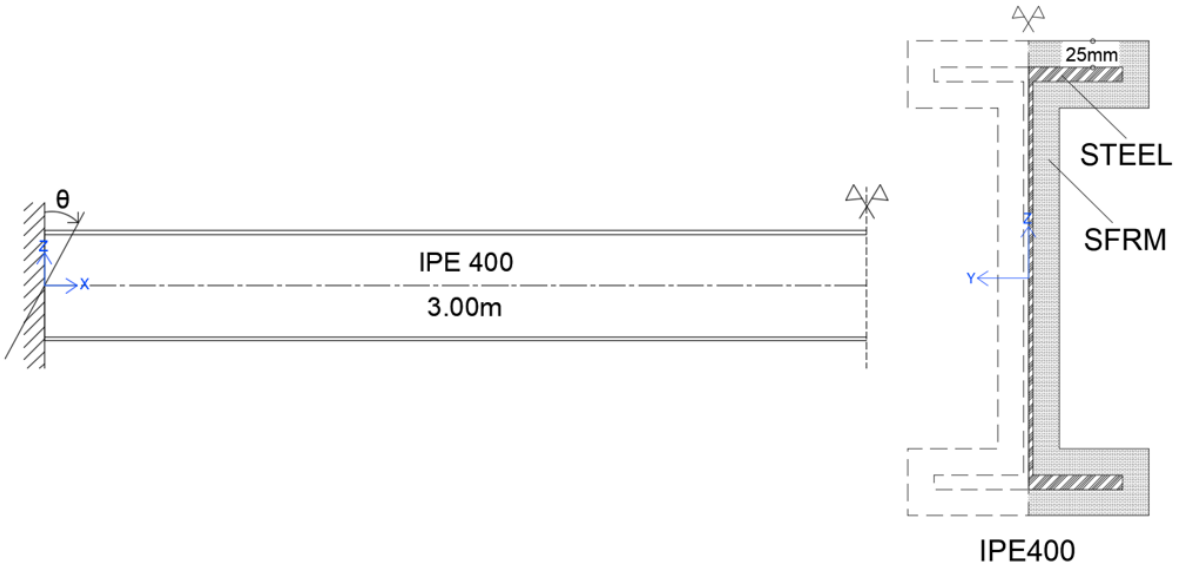

Figure 5. Structural model and cross section

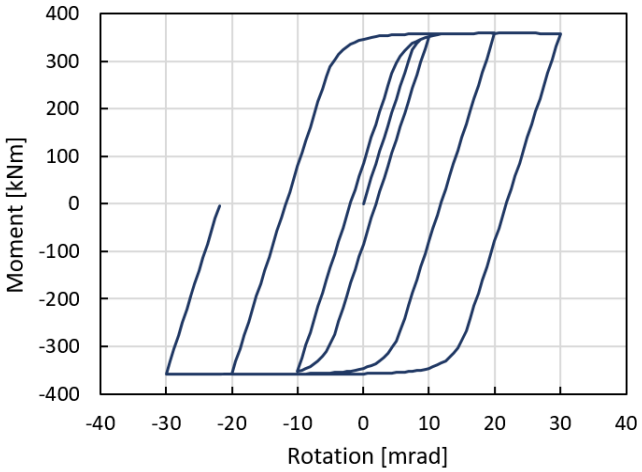

Figure 6. Moment - Rotation curve applied on IPE400 beam

Table 1. Material mechanical properties at normal temperature.

Steel	E	v	E_p	f_y		
	210 GPa	0.3	0 MPa	275 MPa		
Cementitious coating	E	v	E_s	f_t	f_c	β
	40.33 MPa	0.2	5 MPa	0.05 MPa	0.59 MPa	0.05
Interface	S_n			S_t		
	0.04 MPa			0.07 MPa		

E=Elastic modulus, v=Poisson's ratio, E_p=Hardening slope, f_y=Yield stress, E_s=Softening slope, f_t=Ultimate tensile stress, f_c=Ultimate compressive stress, β=Shear retention factor, S_n=Normal bonding strength, S_t=Shear bonding strength

Interface failure

The first failure mode that occurs during the structural analysis is at the interface between the two materials. Delamination develops at the initial steps of the imposed rotation, which initiates at the flanges and mainly on the compression side of each flange. As the rotation increases, delamination spreads on the compression side of both flanges. At a rotation of 1mrad delamination starts developing on the web near the support and gradually spreads towards the midspan of the beam. The part of the beam that exhibits the lowest rate of delamination is the tension side of both flanges. At the end of the first half cycle (rotation = 10mrad) only a small part of the coating at the web near the middle of the beam remains glued to the steel section. At a rotation of 20 mrad, almost all the coating has delaminated from the beam. The delamination pattern at various levels of imposed rotation is displayed in Figure 7.

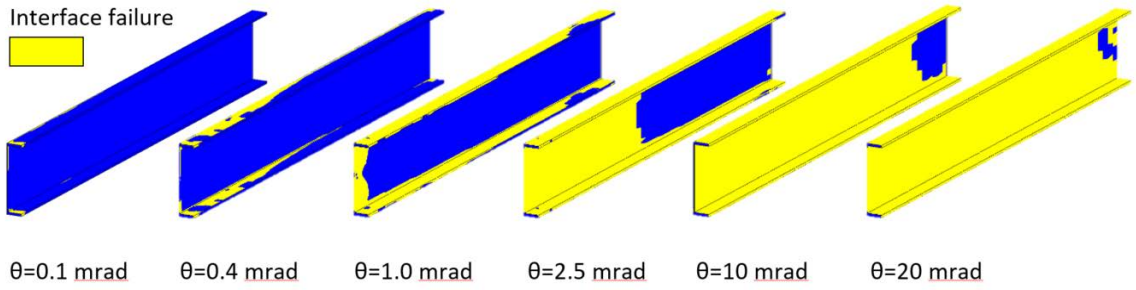

Figure 7. Evolution of interface failure against imposed rotation

Structural damage of the SFRM coating

A quantity that can act as an indicator of the damage the SFRM coating has sustained at the position of the plastic hinge is the cracking strain that has developed in the elements. It is assumed that after the stress – strain curve has reached the end of the softening branch (cracking strain = 0.01) the element has sustained considerable cracking and at that point its fire protection properties are compromised. The evolution of the cracking strain in the cementitious SFRM coating is given in Figure 8 for the peak values of imposed rotation at each loading cycle (-10,-20,-30 mrad) and at yield rotation of -7.3mrad. It can be observed that as the imposed rotation increases, the area of the damaged SFRM coating extends further and affects the flanges and part of the web. The area that is more affected is the SFRM around the flange in tension (upper flange). The material on the compression flange has, also, regions with cracking strain >0.01, because of the tension that develops perpendicular to the compression direction. At yield rotation, only a small area near the end cross section in tension has sustained considerable cracking strain.

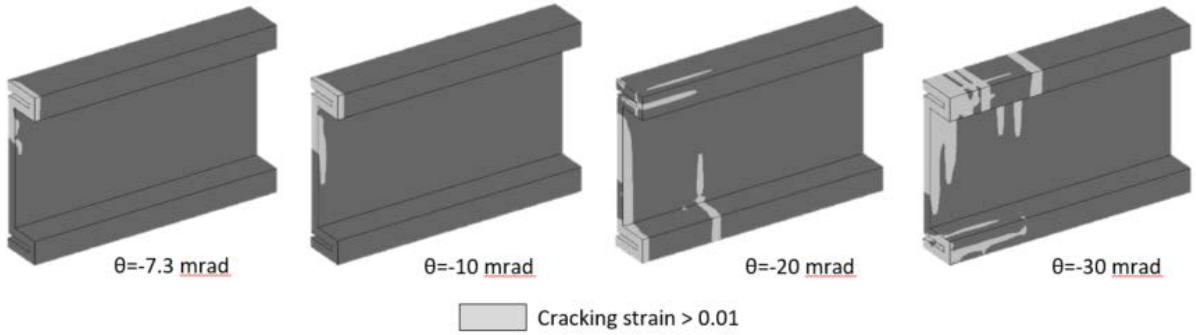

Figure 8. Evolution of SFRM coating damage (cracking strain) against imposed rotation

5. THERMAL NUMERICAL ANALYSIS OF STEEL BEAM WITH SFRM COATING

5.1 Thermal Numerical Model

The second stage of the study is the thermal analysis of the steel beam with the damaged SFRM coating at the position of the plastic hinge and the evaluation of the temperature distribution along the beam, under a 2-hours ISO-834 thermal load. The damage considered in the SFRM coating is caused by a -30mrad rotation, which is the peak value in the last half cycle. At this point, all the SFRM elements that have sustained an average cracking strain >0.01 are considered to have their fire protection capability compromised and are removed from the numerical model, leaving some parts of the steel cross section at the area of the plastic hinge completely or partially exposed to the thermal load. For reference, a steel beam with intact SFRM coating and also a beam without any fire protection are simulated.

The thermal model consists of the IPE400 steel beam with or without the SFRM coating, enclosed between three heat emitting surfaces (Figure 9) that simulate the surrounding air, subjected to the ISO-834 temperature-time history.

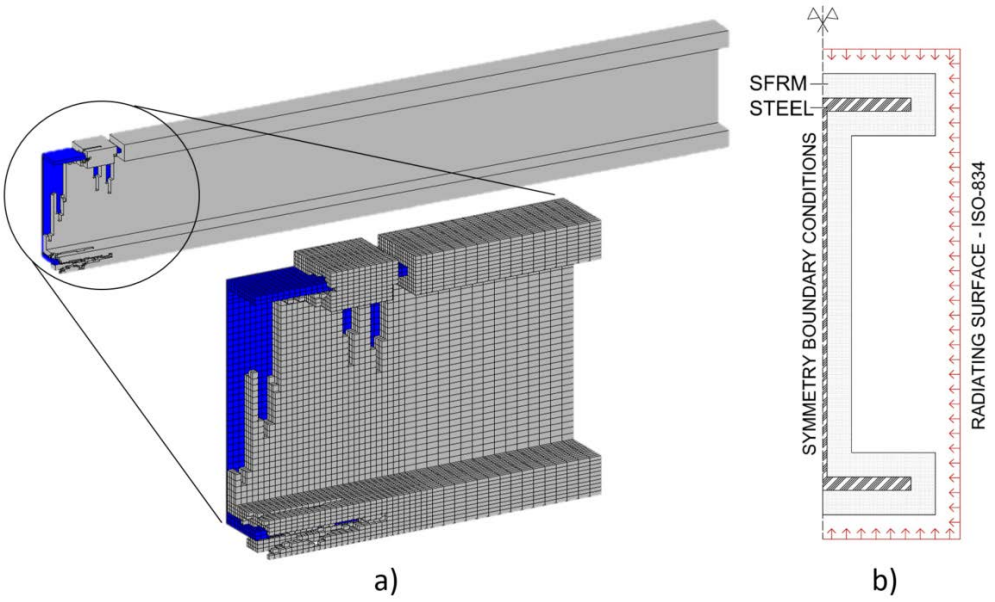

Figure 9. a) Model of the beam with partially damaged SFRM coating at the area of the plastic hinge, b) Thermal model and boundary conditions

Heat is transferred from the source to the beam trough convection and radiation. Natural convection is modelled by a surface film applied on the corresponding exposed SFRM coating or exposed steel opposite the radiating areas, using a heat transfer coefficient for air, of 25 W/m^2·°K. Radiation is modeled between the source radiating surface (emissivity=1) and the target, taking into account the corresponding view factors for every individual element. In the case where the SFRM coating is present, the heat is transferred through conduction from the heated exterior insulation to the steel section. At the interface, the two materials are considered to have the same temperature. Adiabatic boundary conditions are applied at the end cross section, the beam's support, at the midspan of the beam and at the symmetry xz plane. The guidelines of EC3, Part 1-2 (EN 1993-1-2, 2005) were adopted for the thermal properties of steel in elevated temperatures. Regarding the cementitious SFRM coating, the thermal properties are given in Table 2.

Table 2. SFRM thermal properties.

Temperature [°C]										
25	50	100	200	300	400	500	600	800	1000	1200
Thermal Conductivity [W/(m·K)]										
0.0534	0.0745	0.0921	0.0895	0.1057	0.1362	0.1689	0.2156	0.2763	0.3708	0.4081
Specific Heat Capacity [J/(kg·K)]										
801.6	868.4	708.4	925.4	1084.7	1147.5	1255.3	1299.1	1369.6	1411.3	1461.3
Emissivity						**Density [kg/m^3]**				
0.85						313.7				

5.2 Thermal Analysis Results

The temperature evolution under the 2-hours ISO-834 thermal loading and the temperature distribution along the length of the steel beam are presented in Figures 10 and 12. The maximum local temperature time history for the damaged, undamaged and unprotected steel beam are given in Figure 11, where it is shown that the temporal temperature evolution is much slower for the protected beam than for the damaged and the unprotected ones. The partial absence of fire protection leads to a temperature rise that is quite similar to the completely unprotected beam. According to ASTM E119 (1998), the single point maximum temperature failure criterion for steel beams is 704°C above initial conditions. This local temperature is reached for the protected beam in 90 mins, while for the unprotected beam in 18 mins and for the partially damaged beam in 24 mins.

The temperature distribution for the undamaged and the unprotected beams is constant along the length of the beam over the 2-hours, with a slight difference between the web and the flanges. However, in the case of the partially damaged SFRM coating, the temperature distribution is uneven. The temperature is higher in the area of the missing protection and gradually decreases until it becomes even at a distance of about 0.50m – 0.75m. In most cases, as it can be seen in Fig. 10, the temperature decreases rapidly in a small segment of the beam (of about 0.25m) and can reach differences of 573°C in a distance of 0.60 m. This segment is located at the boundary of the missing fire protection, where a part of the steel beam is directly subjected to the thermal load and the subsequent part is covered by the fire protection.

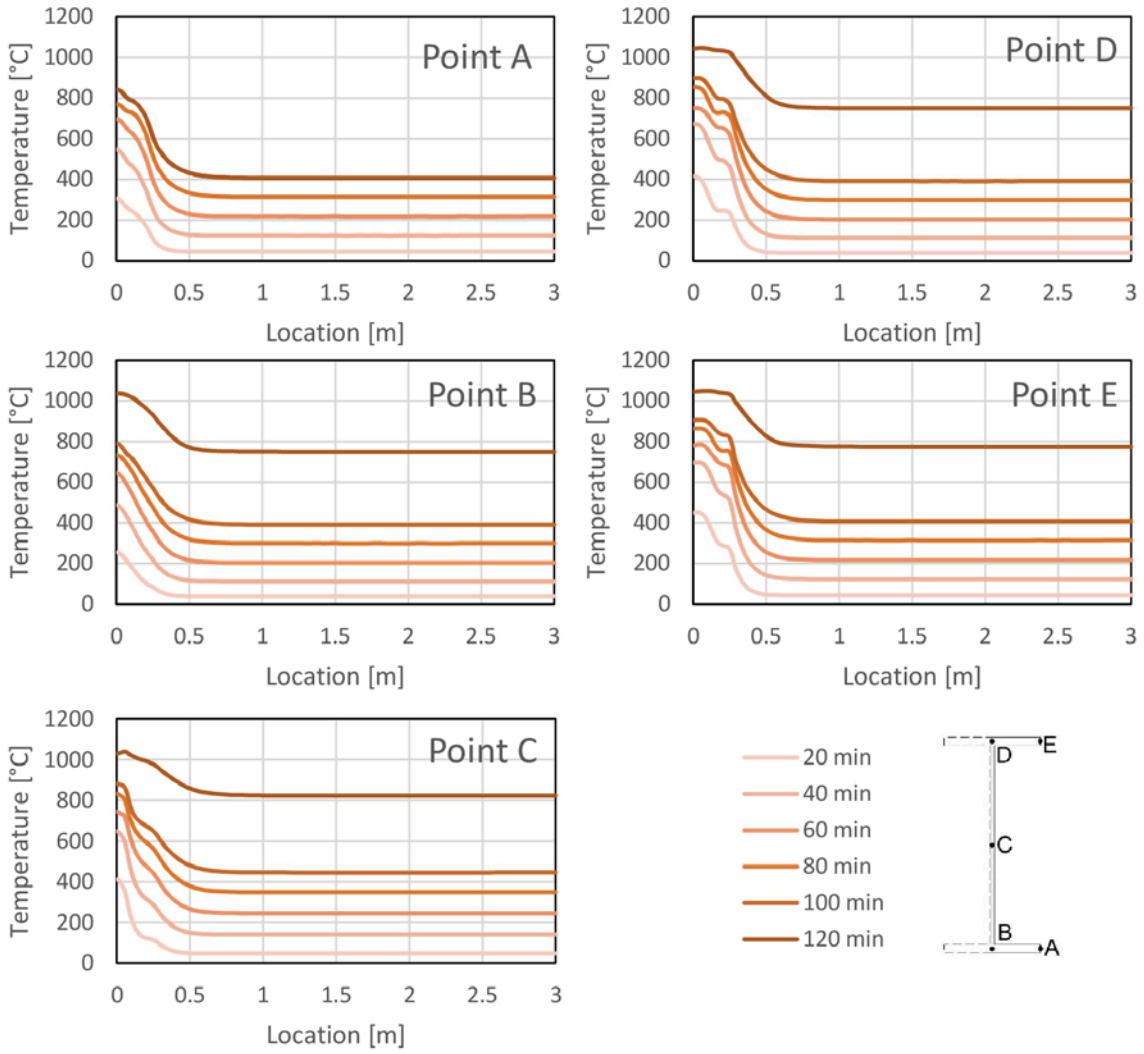

Figure 10. Temperature distribution along the length of the steel beam with the partially damaged SFRM coating

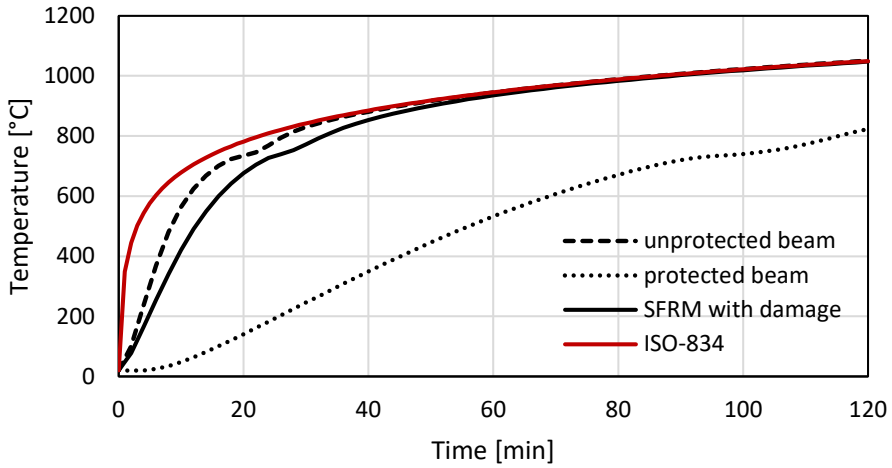

Figure 11. Maximum temperature-time history for the protected, unprotected and partially damaged beam

Figure 12. Temperature distribution along the length of the steel beam with the partially damaged SFRM coating.

6. CONCLUSIONS

Cementitious SFRM coatings, which are widely used for the fire protection of steel structures, due to their low strength can sustain significant damage when the structure is subjected to earthquake loading. The damage of the coating, which consists of both failure of the interface and mechanical failure in the mass of the material, will occur at any position of high deformations, such as the plastic hinges that form in the steel frame. This damage will render the fire protective coating ineffective when the structure is subjected to thermal loads, a common situation in industrial facilities after an earthquake. The partial or complete lack of fire protection will lead to much faster temperature rise in the steel elements and will also cause large temperature differences in the areas close to the position of the missing coating. Uneven temperature distribution can pose a threat for the local and overall stability of the structure, in addition to the degradation of the mechanical strength of steel at elevated temperatures. The current design guidelines do not require damage of fire protection to be taken into account during the design process, but nonetheless, it is an issue that the designer needs to be aware of, during the design, evaluation and retrofitting of steel structures and especially in critical buildings during earthquake events.

7. ACKNOWLEDGMENTS

This study has been funded by the Greek State Scholarship Foundation (IKY) under the action “Scholarship program for post graduate doctoral studies” of the Operational Program "Human Resource Development, Education and Lifelong Learning", 2014-2020 with the co-funding of the European Social Fund (ESF) and the Greek State.

8. REFERENCES

ASTM-119-98, (1998) Standard Test Methods for Fire Tests of Building Construction and Materials, American Society for Testing and Materials, Philadelphia

Braxtan, N. L., and Pessiki, S. P. (2011). Postearthquake Fire Performance of Sprayed Fire-Resistive Material on Steel Moment Frames. *Journal of Structural Engineering*, 137(9), 946–953.

Castiglioni C.A. and Pucinotti R., (2009). Failure criteria and cumulative damage models for steel components under cyclic loading, *J. of Constr. Steel*. Res, 65, 751:765.

Chen, S., Jin, C., & Li, G. Q. (2010). A study on damage mechanism of thick fireproof coating for steel member subjected to monotonic loading, *Proceedings of the 6th International Conference on Structures in Fire* (pp. 130–138). East Lansing, MI, USA.

Chen, S., Jiang, L., Usmani, A., & Li, G. (2014). Damage Mechanisms in Cementitious Coatings for Steel, *Proceedings of the 10th National Conference on Earthquake Engineering*. Anchorage, AK: Earthquake Engineering Research Institute.

"EN 1993-1-2: Design of steel structures - General rules - Structural fire design," European committee for Standardization, 2005.

"EN 1993-1-1: Design of steel structures - Part 1-1: General rules and rules for buildings" European committee for Standardization, 2005

"EN 1998-1-1: Design of structures for earthquake resistance - Part 1: General rules seismic actions and rules for buildings" European committee for Standardization, 2004

"EN 1991-1-1: Actions on structures - Part 1-1: General actions - Densities, self-weight, imposed loads for buildings" European committee for Standardization, 2002

Faggiano, B. and Mazzolani, F.M. (2011). Fire after earthquake robustness evaluation and design: Application to steel structures, *Steel Constr. Des.* Res., 4(3), 183-187.

Keller, WJ. (2012), Thermomechanical response of steel moment-frame beam-column connections during post-earthquake Fire Exposure, *Ph. D Dissertation*, Lehigh University, Bethlehem, Pennsylvania.

Krawinkler, H., (1981). Performance assessment of steel components. *Earthq Spectra*, 3(1), 27:41.

Krawinkler, H., Zohrei, M., (1983). Cumulative damage in steel structures subjected to earthquake ground motion. *Comput Struct*, 16(1-4), 531:41.

Memari. M, Mahmoud. H, Ellingwood, B. (2014). Post-earthquake fire performance of moment resisting frames with reduced beam section connections, J. of Constr. Steel. Res., 103, 215-229.

"MSC-MARC." MSC.Software Corporation, 2014

Pantousa, D. and Mistakidis E., (2015), Fire-after-earthquake resistance of steel structures using rotational capacity limits, *Earthq Struct*,10(4), 867-89

"SAP 2000 Ver. 19.2", Integrated finite element analysis and design of structures basic analysis reference manual. Berkeley (CA, USA): Computers and Structures INC; 2017

Zografopoulou, K., & Mistakidis, E. (2017). Numerical simulation of the behaviour of steel members with damaged SFRM fire protection coatings at elevated temperatures. *Proceedings of Eurosteel 2017*, Ce/papers, 1(2–3), 2688–2697.